


Article

Design and Visual Implementation of a Regional Energy Risk Superposition Model for Oil Tank Farms

Yufeng Yang ¹, Xixiang Zhang ¹, Shuyi Xie ², Shanqi Qu ^{3,4,*}, Haotian Chen ^{3,4,*}, Qiming Xu ^{3,4} and Guohua Chen ^{3,4} 

¹ Institute of Science and Technology, China Oil & Gas Pipeline Network Corporation, Langfang 065000, China; yangyf@pipechina.com.cn (Y.Y.); zhangxx11@pipechina.com.cn (X.Z.)

² State Key Laboratory of Oil and Gas Equipment, CNPC Tubular Goods Research Institute, Xi'an 710077, China; xieshuyi0810@gmail.com

³ Institute of Safety Science & Engineering, South China University of Technology, Guangzhou 510640, China; 202111080757@mail.scut.edu.cn (Q.X.); mmghchen@scut.edu.cn (G.C.)

⁴ Guangdong Provincial Science and Technology Collaborative Innovation Center for Work Safety, Guangzhou 510640, China

* Correspondence: 202321004012@mail.scut.edu.cn (S.Q.); 202321003990@mail.scut.edu.cn (H.C.)

Abstract: Ensuring the safety of oil tank farms is essential to maintaining energy security and minimizing the impact of potential accidents. This paper develops a quantitative regional risk model designed to assess both individual and societal risks in oil tank farms, with particular attention to energy-related risks such as leaks, fires, and explosions. The model integrates factors like day–night operational variations, weather conditions, and risk superposition to provide a comprehensive and accurate evaluation of regional risks. By considering the cumulative effects of multiple hazards, including those tied to energy dynamics, and the stability and validity of the model are researched through Monte Carlo simulations and case application. The results show that the model enhances the reliability of traditional risk assessment methods, making it more applicable to oil tank farm safety concerns. Furthermore, this study introduces a practical tool that simplifies the risk assessment process, allowing operators and decision-makers to evaluate risks without requiring in-depth technical expertise. The methodology improves the ability to safeguard oil tank farms, ensuring the stability of energy supply chains and contributing to broader energy security efforts. This study provides a valuable method for researchers and engineers seeking to enhance regional risk calculation efficiency, with a specific focus on energy risks.

Keywords: energy security; oil tank farm; regional risk model; energy risk; quantitative risk assessment; visualization interface



Citation: Yang, Y.; Zhang, X.; Xie, S.; Qu, S.; Chen, H.; Xu, Q.; Chen, G. Design and Visual Implementation of a Regional Energy Risk Superposition Model for Oil Tank Farms. *Energies* **2024**, *17*, 5775. <https://doi.org/10.3390/en17225775>

Academic Editor: Krzysztof Skrzypkowski

Received: 11 October 2024
Revised: 11 November 2024
Accepted: 13 November 2024
Published: 19 November 2024



Copyright: © 2024 by the authors. Licensee MDPI, Basel, Switzerland. This article is an open access article distributed under the terms and conditions of the Creative Commons Attribution (CC BY) license (<https://creativecommons.org/licenses/by/4.0/>).

1. Introduction

The aggregation of major hazards in the oil tank area significantly increases the risk of fire, explosion, or release of hazardous substances accidents. This poses significant challenges when it comes to the safety assessment of chemical storage facilities. On 3 March 2023, a severe explosion occurred at the oil storage facility of the state-owned Indonesian oil company Pertamina, resulting in extensive damage, the deaths of at least 19 individuals, and injuries to several others [1]. On 1 May 2023, an explosion and fire occurred at the Yanshan Chemical Industry Co., Ltd., a company specializing in the production of oxygen-based materials in Yantai, Shandong, China. The accident resulted in the deaths of 10 individuals and injury to one person [2]. In the event of such an occurrence, the immediate vicinity and surrounding infrastructure may be severely damaged, potentially leading to a cascading series of accidents [3]. Changes in injection and extraction pressures, along with various imbalance factors in oil product tank areas, combined with the external environmental corrosion of processing equipment and the impact of human factors on piping and equipment, can easily compromise the integrity of oil stations. If leaks occur in

pipelines, tanks, or other facilities, they can quickly lead to fires and explosions. Furthermore, the wastage of oil and gas resources and the environmental pollution resulting from widespread oil tank leaks pose significant threats to sustainable development [4]. Consequently, conducting a comprehensive risk assessment for chemical facilities, particularly one that considers the cumulative impact of multiple hazards, is of paramount importance for the scientific planning of safe and effective regional safety strategies.

Quantitative risk assessment techniques have been increasingly used in numerous risk management decisions. It is particularly important to develop effective risk assessment methods, especially in highly populated and industrialized areas [5]. The current research in the field of Regional Quantitative Risk Assessment can be broadly divided into two main areas. First, the development and optimization of models for predicting the probability of major accidents and assessing their consequences. This includes the creation of models for specific types of accidents, such as fires and explosions, as well as the development of models for estimating the impact of such accidents. Zhang, H.Y. et al. investigated the thermal radiation characteristics of hydrogen jet fires, revealing the significant effects of the leak's diameter and pressure on thermal radiation. Their findings provide critical support for the accurate assessment of hydrogen jet fire risks [6]. Jie Su et al. systematically quantified regional risk relationships based on Bayesian rules and the law of total probability, conducting an in-depth study of the transmission relationships within regional risks [7]. Lee, K. et al. utilized DNA PHAST (Version 8.9) to generate quantitative data on the effects of a fire and explosion in a single blast event [8]. Second, there is a focus on understanding the cascading effects of accidents, which can be caused by a range of factors, including thermal radiation, pressure waves, and the dispersion of fragments. The second core indicator is the calculation of individual risk and societal risk. Major authorities, such as the Dutch Ministry of Environment and the UK Health and Safety Executive, have established differentiated individual risk standards based on regional characteristics and the actual conditions of the equipment in question [9]. Park, B. et al. used the RISKCURVES software (Gexcon, Norway) package to quantify the risks to the environment and (petroleum) chemical facilities posed by the storage and transportation of hazardous substances to surrounding populations and structures [10]. Kwak, H. et al. conducted a quantitative risk assessment using DNV SAFETI (Version 8.9) for hydrogen refueling stations operating at high pressures, demonstrating their safety [11]. Abdolhamidzadeh, B. et al. employed the Monte Carlo simulation method to investigate the differences in individual risks associated with single and multiple hazard sources [12]. Zhao, M. et al. developed a tool called RiskUMH (risk of urban major hazards) using GIS geoprocessing technology, effectively integrating emerging GIS techniques with risk assessment methods into a unified toolbox [13]. The approach of Rajeev et al. involved the integration of three key elements: scenario, frequency, and consequence information [14]. This allowed for a more detailed calculation of individual risks, expressed as the annual probability of death within a specified distance of a hazardous source. Tahmid et al. employed a geographical information system to assess the vulnerability and risk level of human and societal systems to chemical accidents [15]. The studies conducted by Rajeev et al. and Tahmid et al. have differing focuses but are nevertheless united in their objective of developing and applying risk assessment models [14,15].

While previous research has significantly contributed to the visual representation of accident impacts within a defined area, there remains a need for more granular subdivisions of regional accident risk levels. Further investigation is also required to deepen the understanding of how accidents influence risk assessment processes. In practical applications, several critical challenges have become evident. One notable limitation in calculating comprehensive regional risk is the large number of grid-based processing steps involved, particularly the intersection of accident consequence severity with occurrence probability, followed by the risk calculation for each grid. This process is often laborious, time-consuming, and prone to human error. Moreover, conventional risk assessment tools tend to require substantial financial investment and present a steep learning curve, limiting

their accessibility and utility. Thus, there is a pressing need for a standardized, efficient, and user-friendly risk calculation tool to facilitate the risk assessment process, particularly in high-stakes environments such as oil tank farms, where energy security is paramount. This study seeks to address these gaps by developing a detailed individual and societal risk assessment model, which integrates visual risk mapping to depict risk distribution across large oil tank farm areas. By generating individual risk equivalence lines and societal risk curves, this model offers a more precise and intuitive understanding of regional risk patterns. A case study of an oil tank accident, evaluated against the acceptable risk standards of the chemical industry, serves to validate the model's practical application. This work aims to provide a scientific basis for the management of energy infrastructure and support informed decision-making during emergency situations. By enhancing the accuracy and efficiency of regional risk assessments, this study contributes to improved risk management practices in oil tank farms, ultimately reinforcing broader energy security efforts.

2. Basic Model

2.1. Individual Risk Calculation Model

Individual risk is the frequency of exposure to hazards for unprotected persons at a particular location [16]. Individual risk has distinct geographic attributes and is visualized as risk contours at different levels on a geographic map in a regional risk assessment, which marks a specific level of risk shared by points within a region, rather than being specific to a particular individual. This paper calculates the individual risk for each grid point.

The methodology for determining individual risk at a grid point is outlined in Figure 1. It starts by selecting the frequency of a loss of containment (LOC) event (f_s). After this, a weather class “ M ” and a wind direction “ ϕ ” are chosen, considering both day and night divisions, with conditional probabilities represented as P_M and P_ϕ . Once the weather and wind parameters are set, the next step is to select an ignition event, applicable only to flammable substances, with its conditional probability denoted as P_i . This step determines whether an ignition occurs, influencing the severity of the consequences. The iterative process continues by determining the contributions of various factors to the individual risk at the grid point, according to Equation (1). If all possible ignition events, weather classes, and wind directions have been considered, the contributions are summed to obtain the total individual risk at the grid point, according to Equation (2). The leakage probability of equipment and facilities is determined in accordance with GB/T37243-2019 (Determination method of external safety distance for hazardous chemicals production units and storage installations) [17], and SH/T 3226-2024 (Standard for quantitative analysis of petrochemical process risk) [18], which define leakage scenarios and frequencies. To determine the probability of ignition, AQ/T3046-2013 (Guidelines for quantitative risk assessment of chemical enterprises) [19] provides recommended values, and an appropriate reference value can be selected based on the requirements of the risk assessment method.

$$\Delta IR_{S,M,\phi,i} = f_s \times P_M \times P_\phi \times P_i \times P_d (y^{-1}) \quad (1)$$

$$IR = \sum_S \sum_M \sum_\phi \sum_i \Delta IR_{S,M,\phi,i} \quad (2)$$

where f_s is the frequency of a loss of containment, P_M is the probability of a weather class, P_ϕ is the probability of obtaining a wind direction, P_i is the conditional probability of an ignition event, and P_d is the individual lethality probability.

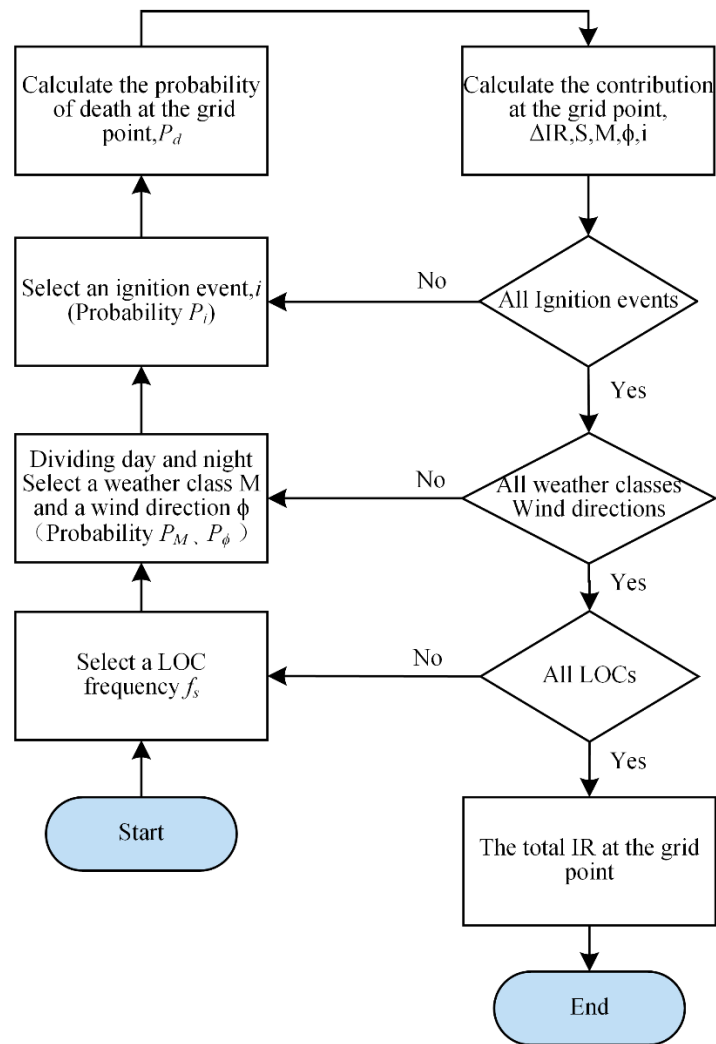


Figure 1. Procedure for calculating individual risk IR at grid points.

The individual lethality probability P_d is calculated according to Equations (3) and (4).

$$P_d = 0.5 \times \left[1 + \operatorname{erf} \left(\frac{P_r - 5}{\sqrt{2}} \right) \right] \quad (3)$$

$$\operatorname{erf}(x) = \frac{2}{\sqrt{\pi}} \int_0^x e^{-t^2} dt \quad (4)$$

The changing probit variable of a person under overpressure is calculated by Equation (5),

$$P_r = -10.462 + 1.35 \times \ln(P_s) \quad (5)$$

where, P_s is the overpressure, bar.

The individual lethality probability of a person exposed to thermal radiation is determined using different ellipses in Figure 2, each representing varying radiation intensities as calculated by DNV SAFETI (Version 9.0) [20]. The highest radiation intensity is observed in the central area, where the lethality reaches 1.0, indicating that almost all individuals within this zone will not survive. As the distance from the center increases, both radiation intensity and lethality decrease accordingly. Figure 2 shows that radiation intensity is greatest within the innermost ellipse, while outside the outermost ellipse, the radiation level drops to zero. Between these ellipses, the corresponding lethality probability is calculated through interpolation of the specific radiation intensities.

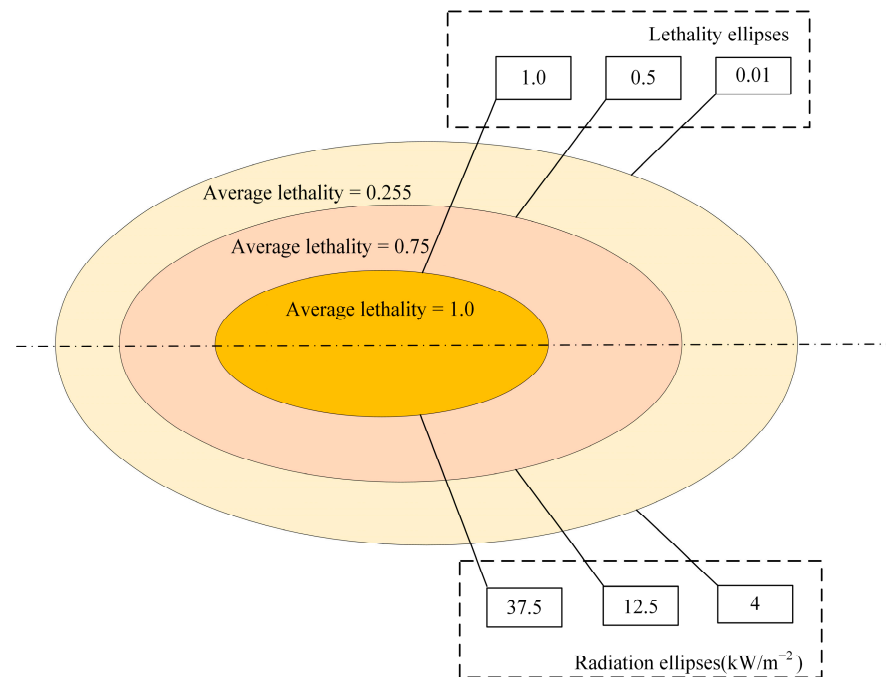


Figure 2. Interpolation between radiation ellipses and the corresponding probabilities of lethality.

2.2. Societal Risk Calculation Model

Where a population is exposed to risk, a simple aggregation of the individual level of risk by multiplying by the population exposed does not reveal all the possible risks [21]. Therefore, the concept of societal risk needs to be introduced. Societal risk is the relationship between the probability of an accident occurring and the number of accident casualties [16]. ISO 31000 defined societal risk as the relationship between the frequency of occurrence of a consequence (F) and the number of people bearing the consequences (N). Societal risk possesses numerous measures [22]. ISO 31000 provides the most commonly used characterization method, the *F-N* curve, which helps to understand the consequences of risk and its causes and provides a basis for management decisions. This paper primarily focuses on the consequences of leakage in large atmospheric oil tanks, where the storage medium is crude oil, a flammable substance. Therefore, Equation (6) is used to determine the frequency of leakage accident consequences in large oil storage tanks, denoted as *F*.

$$F = f_s P_o \tag{6}$$

where *P_o* is the probability of an accident consequence.

The value of *P_o* varies with the type of release, the state of the material, the type of ignition, and the type of accident. As shown in Table 1, DNV SAFETI v.9.0 analyzed the effect of these factors on the value of *P_o* using an event tree [20].

N_{edf|o} is the total number of fatalities in the accident. It is obtained by summing the number of fatalities calculated from all grids, as shown in Equations (7) and (8), and the gridding of the area risk in question, which will be mentioned later.

$$N_{x,y|o} = N_{x,y} \bar{P}_{d, FN, x,y|o} \tag{7}$$

$$N_{edf|o} = \sum_{\text{All calculation squares}} N_{x,y|o} \tag{8}$$

where *N_{x,y|o}* is the number of fatalities per grid cell centered on *x,y*, *N_{x,y}* is the number of people within the grid cell centered on *x,y*, and *P_d* is the probability of death of a person per grid cell centered on *x,y*.

Table 1. Table of values for the probability of accident consequence P_o .

Event Tree	Branch 1	Branch 2	Branch 3	Branch 4	P_o
	Independent BLEVE				P_b
	Independent Pool Fire				$P_{wss}P_p$
Continuous release, No Rainout	Immediate	BLEVE Explosion			$P_sP_{wss}P_{bl}P_i$ $P_sP_{wss}P_eP_i$
	Not immediate	Delayed ignition	Explosion		$(1 - P_i)P_{wss}P_eP_{di}$
Instantaneous release, No Rainout	Immediate	BLEVE Explosion			$P_{wss}P_bP_i$ $P_{wss}P_eP_i$
	Not immediate	Delayed ignition	Explosion		$(1 - P_i)P_{wss}P_eP_{di}$
Continuous release, Rainout	Immediate	Not short	Pool fire		$(1 - P_s)P_{wss}P_i$
		Short release	BLEVE and pool fire		$P_sP_{wss}P_{tp}P_i$
		BLEVE alone		$P_sP_{wss}P_{bl}P_i$	
		Explosion and pool fire		$P_sP_{wss}P_{ep}P_i$	
		Explosion alone		$P_sP_{wss}P_eP_i$	
		Pool fire alone		$P_sP_{wss}P_pP_i$	
	Not immediate	Dispersion Residual	Delayed Pool fire	Explosion	$(1 - P_i)P_{wss}P_eP_{di}$ $(1 - P_i)P_{wss}P_{rp}P_{irp}$
Instantaneous release, Rainout	Immediate	BLEVE and pool fire			$P_{ws}P_{tp}P_i$
		BLEVE alone			$P_{ws}P_{bl}P_i$
Explosion and pool fire				$P_{ws}P_{ep}P_i$	
Explosion alone				$P_{ws}P_eP_i$	
		Pool fire alone			$P_{ws}P_pP_i$
	Not immediate	Dispersion Residual	Delayed Pool fire	Explosion	$(1 - P_i)P_{ws}P_eP_{di}$ $(1 - P_i)P_{ws}P_{rp}P_{irp}$

After completing the modeling of F and N , the next step is to construct the F - N curve. As shown in Figure 3, constructing the F - N curve mainly includes ten steps:

- (1) Grid the risk area at an appropriate density.
- (2) Determine the weather conditions in the region and the frequency of leaks from each tank.
- (3) Consider all the types of accidents that may occur in the region and add data on the consequences of the accidents, such as thermal radiation, explosion overpressure, etc., to the grid.
- (4) Select one of the weather classes.
- (5) Select one of the accident types that may occur in that weather class.
- (6) Select a grid and calculate the probability of death P_d based on the consequences of the accident, and then get the number of fatalities $N_{x,y|o}$ in a single grid point.
- (7) Repeat steps (4)–(6) until all grid deaths have been calculated.
- (8) Add up all the grid fatalities to get the total number of fatalities N .
- (9) Calculate the frequency F of the accident.
- (10) Repeat steps (4)–(9), considering all weather classes, wind directions, and accident types. Use the calculated N and F to plot the F - N curve.

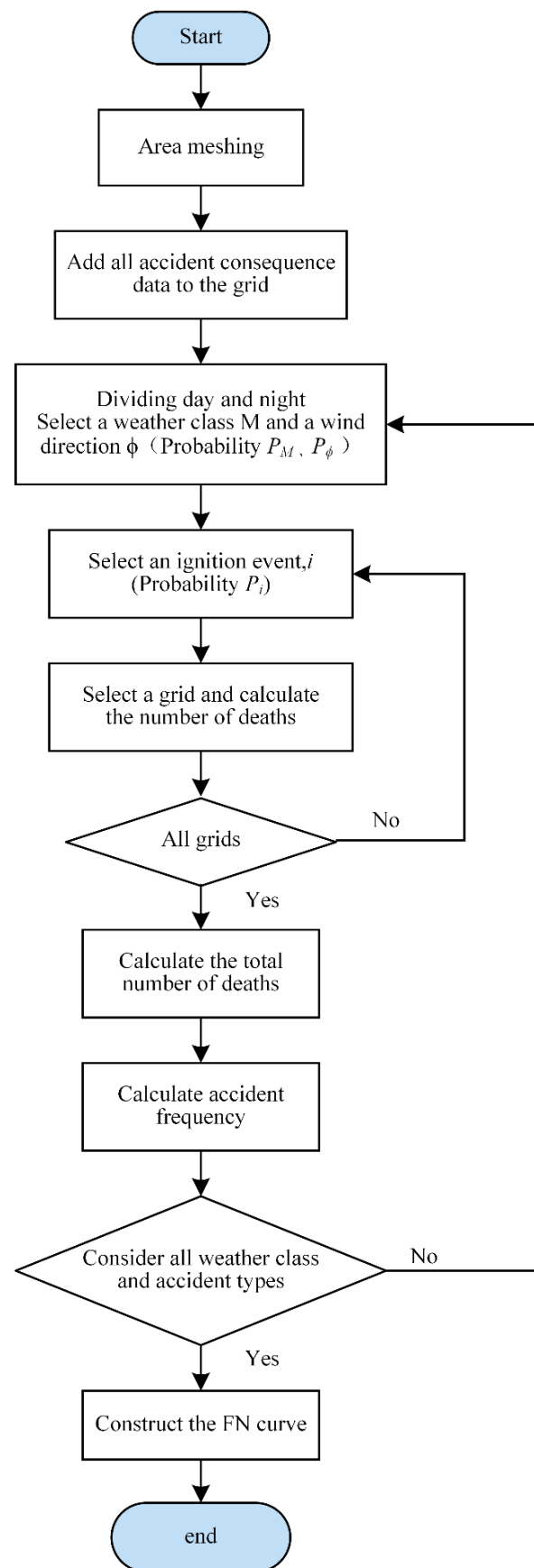


Figure 3. *F-N* curve plotting process.

3. Methods

The methodology of this study comprises four interconnected steps. First, the assessment's scope and objectives are defined, guiding data collection and scenario construction. Next, essential data are gathered, including storage medium properties, tank specifications, and meteorological and geographic information, which serve as the foundation for scenario development and calculations. Following this, accident scenarios are created based on the defined objectives and collected data, and appropriate computational models are selected for analysis, providing detailed inputs for program development. Finally, all input data and scenario models are integrated into the program for calculations. The results, including risk distribution and curves, are presented through a visual interface, allowing users to clearly understand the risk assessment outcomes.

3.1. Design Process

3.1.1. Evaluation Objectives and Data Collection

The design process for risk assessment in oil product tank farms begins with defining the objectives and scope of the assessment, including the number and layout of storage tanks, the location of surrounding facilities, and environmental conditions. Normally, gasoline and diesel are relatively stable substances, and the primary type of accident following a leakage is a fire [23]. By identifying the sources of risk, a foundation is established for subsequent accident analysis. Both internal data, such as the characteristics of the storage medium (e.g., flash point, ignition point) and the physical properties of the tanks (e.g., material, dimensions, fill rate), and external data, including meteorological conditions (e.g., wind speed, wind direction, day–night temperature variations) and geographical information (e.g., topography, distribution of neighboring facilities), must be collected. These data are typically derived from historical accident records, equipment maintenance logs, and environmental monitoring results, and the quality of the data directly influences the reliability of the assessment results. During the data collection stage, pre-processing—such as handling outliers and converting data formats—is necessary to ensure accuracy. The processed data are then used as inputs for models that support the construction and calculation of accident scenarios.

3.1.2. Accident Scenario Construction

Once the data are prepared, accident scenarios are constructed to analyze potential types of accidents (e.g., leaks, pool fires, explosions). Various scenarios are developed based on the actual data. For each scenario, appropriate computational models are selected for analysis. For instance, in the case of thermal radiation from pool fires, a solid flame model is employed to calculate radiation intensity by inputting parameters such as combustion rate and flame emissivity. In gas cloud explosion scenarios, the TNO multi-energy method is applied to predict explosion overpressure, taking into account factors like explosion intensity and the distance between the explosion source and the target. These calculations are executed through programming to ensure both the efficiency and accuracy of the models.

3.2. Program Development

3.2.1. Individual Risk Architecture

The individual risk calculation process is articulated through a modular framework, implemented using MATLAB App Designer (MATLAB 2023b). The first module focuses on tank parameters, considering critical aspects such as pressure, temperature, and the nature of the substance stored. This module assesses the probability of fatality for individuals in the event of an accident, establishing a fundamental determinant of individual risk. Following this, the weather factors module introduces the probabilities of various meteorological conditions, examining their influence on the dispersion and consequences of accidents. For example, wind speed and direction can significantly affect how hazardous materials spread, impacting the risk zones for individuals. The final module, dedicated to plotting, creates contour maps that visually represent the risk levels in the vicinity of the tanks,

where each contour line corresponds to a specific risk value. This visualization is essential for understanding how risk fluctuates with distance from the source. Ultimately, the main function synthesizes the results from these modules, culminating in a thorough assessment of individual risk. The entire application is designed with user interaction in mind, allowing for real-time data input and visual feedback through the MATLAB App Designer interface.

In conducting a risk assessment of an oil tank farm, the core of the risk calculation relies on a detailed consequence analysis of the accident scenario. As illustrated in Figure 4, this process requires the input of several key parameters (Refer to Appendix A, Table A1): failure frequency f_s , immediate ignition probability P_i , thermal radiation and overpressure matrices (early pool fire thermal radiation matrix E , late pool fire thermal radiation matrix L , explosion overpressure matrix O), weather parameters including wind direction and daytime and nighttime wind frequency (P_{day} , P_{night}), and mapping parameters such as grid size G_s and grid step. The system automatically integrates these inputs and executes a complex computational algorithm to generate an $i \times i$ matrix. This matrix simulates and quantifies the probability of fatal injuries to individuals at different locations under specific conditions, P_d , through iterative calculations, where each cell represents a risk state based on various factors such as leakage source location, wind direction, and wind speed. To visualize and present the calculation results, the program presents the user-input data in a tabular format and supports hierarchical data analysis, enabling the comparison of risks across different storage tanks. Additionally, the program generates statistical tables that are further analyzed using contour plots, providing a detailed assessment of individual risks at each grid point.

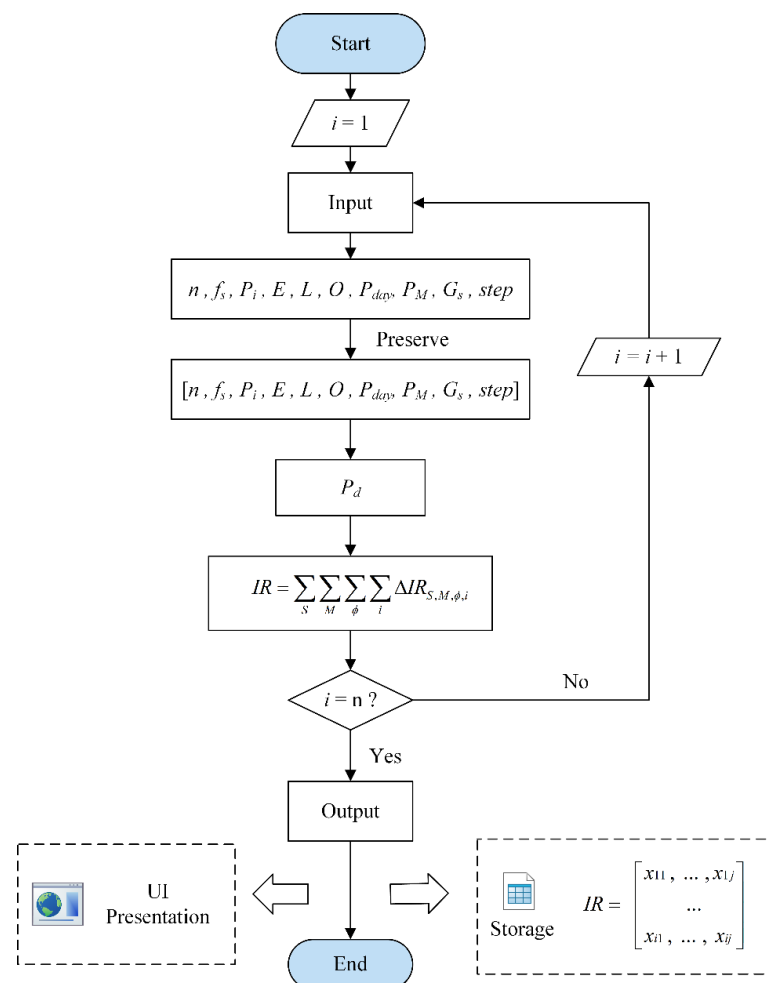


Figure 4. Individual risk matrix calculation.

The primary methods of assessing pool fires include point source methods, solid flame modeling, and computational fluid dynamics (CFD) methods, with the solid flame and CFD methods being predominantly recommended in the relevant standards. The CFD model of fire-driven fluid flow is specifically included in the U.S. Federal Safety Standards for evaluating thermal radiation from LNG plants [24]. Gansu Shen et al. [25] proposed an improved solid flame model. This model corrects the flame diameter by considering flame height and flame volume. The improved model can better predict thermal radiation from heptane pool fires. It works effectively in both the near and far fields. In this study, the solid flame model was selected for calculating thermal radiation consequences, and the calculations were implemented through custom code.

The main methods of calculating gas cloud explosion loads include the TNT equivalent method, BST method, TNO multi-energy method, and computational fluid dynamics (CFD) method. The TNT equivalent method estimates the explosion load by equating the energy released from a gas explosion to an equivalent amount of TNT and predicting the explosion effect based on TNT explosions. However, due to the significant difference in energy release rates between TNT explosions and gas cloud explosions, the TNT equivalent method is unsuitable for predicting gas explosion overpressure. The BST and TNO multi-energy methods predict explosion overpressure based on similar principles, both requiring the selection of an explosion intensity curve, followed by determining the overpressure according to the distance between the explosion source and the target point. The BST method takes into account factors such as flame propagation constraints, obstacle density, and fuel reactivity, using these to determine flame propagation speeds and select the corresponding explosion wave intensity curve. The TNO multi-energy method incorporates factors such as ignition source strength, explosion blockage, and constraint levels into its explosion intensity rating. Tsukada et al. studied and implemented the TNO explosion load prediction method to calculate combustible cloud volumes associated with predefined overpressure values [26]. Therefore, in this paper, the TNO multi-energy method was chosen to calculate the consequences of explosion overpressure shockwaves, and the calculations were implemented through custom code.

This study primarily analyzes the effects of pool fires and explosions resulting from oil tank leaks, with calculations for thermal radiation intensity and explosion overpressure values conducted using MATLAB 2023b. The calculations for thermal radiation and explosion overpressure were performed separately, and their results were incorporated as input parameters for the assessment of individual risk. This comprehensive approach ensures a thorough evaluation of potential hazards associated with oil tank leaks. During the computation process, given the potential for a large number of tanks, the program incorporates a mechanism to accumulate and sum the results of each iteration, ensuring efficient handling of consequence accumulation even with a high number of tanks. Additionally, the calculation process is optimized into two stages: one dedicated to cumulative summation and the other to direct algebraic operations, further enhancing computational efficiency.

3.2.2. Societal Risk Architecture

In contrast to the individual risk assessment, the societal risk assessment considers the impact of the consequences of the BLEVE fireball accident. The TNO fireball method is one of the most commonly used models for calculating thermal radiation from the BLEVE fireball [22]. Therefore, in this paper, the TNO fireball method is used to calculate the thermal radiation consequences.

As shown in Figure 5, the input parameters of societal risk include (Refer to Appendix A, Table A1): the failure frequency (f_s), population matrix (*population*), immediate ignition probability (P_i), thermal radiation and explosion overpressure matrices (early pool thermal radiation matrix (E), late pool thermal radiation matrix (L), explosion overpressure matrix (O), BLEVE thermal radiation matrix B), weather parameters (daytime and nighttime wind direction and frequency P_{day} , P_{night}), and mapping parameters (grid size G_s , grid *step*). Similar to the individual risk calculation, the societal risk visualization

interface stores the user input parameters in the form of tables, which are called in the background to calculate the number of fatalities (N) and frequency (F) for different weather levels (M), wind directions (ϕ), and ignition events (i). After completing the calculations for all accident types, an $I \times 2$ F - N matrix is obtained. Sorting the matrix by N values in ascending order, the F values are cumulatively added row by row to calculate the frequency for accidents with more than N fatalities. This process is repeated until the last row, resulting in an F - N matrix where F decreases as N increases. Finally, the F - N curve can be obtained by plotting the corresponding N and F in the matrix on the logarithmic scale.

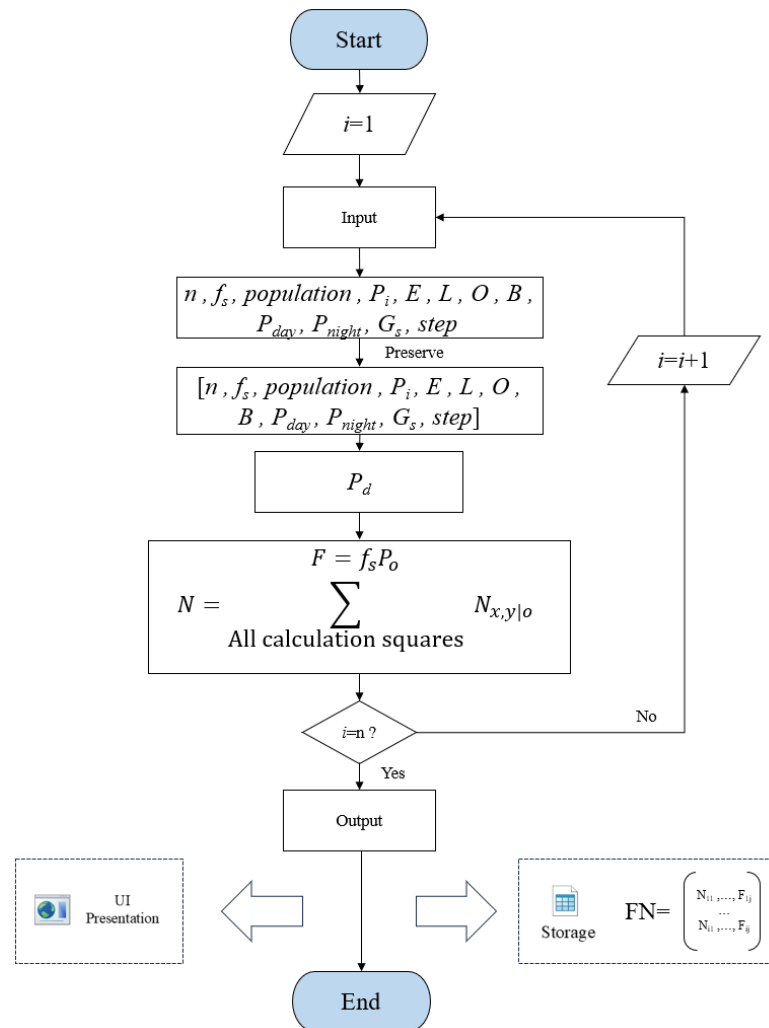


Figure 5. Societal risk matrix calculation.

3.3. Outcome Visualization

The user interface (UI), as shown in Figures 6 and 7, consists of three input modules for collecting consequence parameters, weather conditions, and plotting preferences, respectively, along with a results display panel. The results panel intuitively presents individual risk contour plots and F - N curves, while also integrating a data export function. Additionally, it supports the simultaneous display of graphs and tables, meeting user needs for comprehensive analysis and reporting.

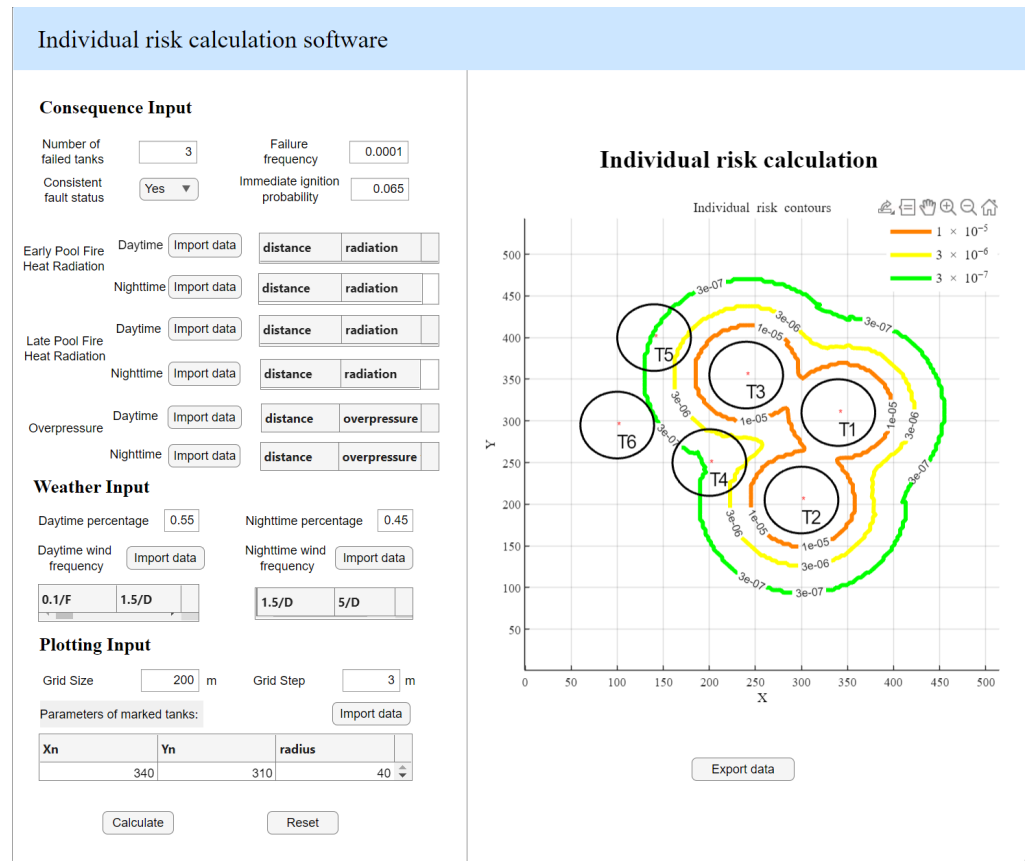


Figure 6. Calculation interface and contour distribution of individual risk for an oil tank farm.

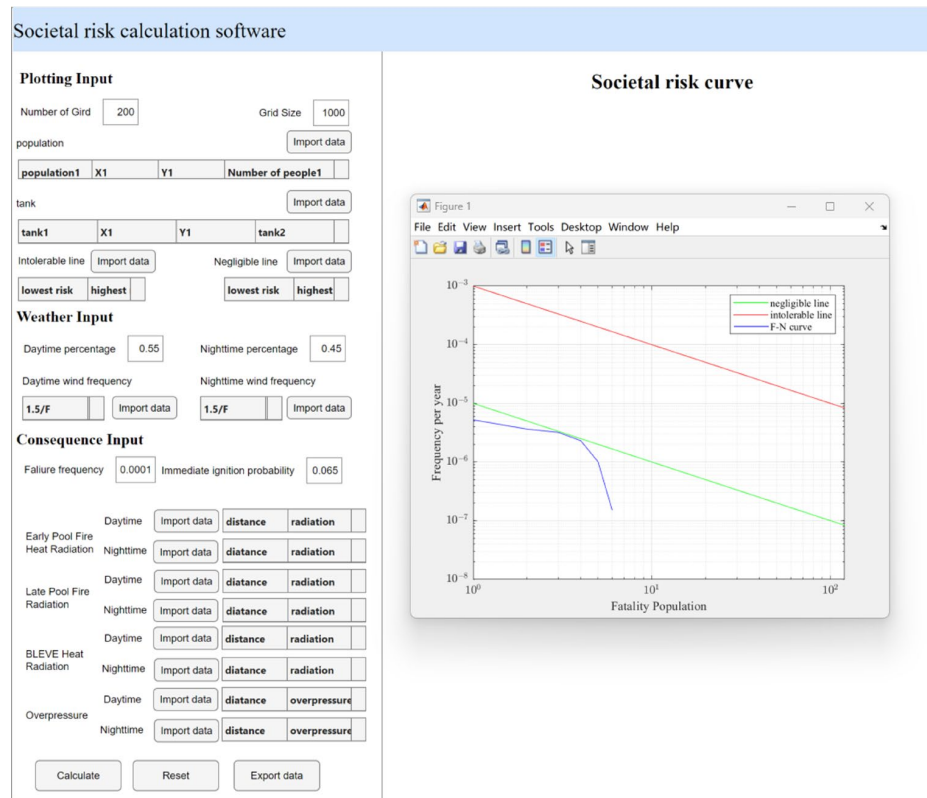


Figure 7. Calculation interface and F-N curve of societal risk for an oil tank farm.

According to the Chinese Standard GB 36894-2018 (Risk criteria for hazardous chemicals production unit and storage installations) [27], Table 2 provides color-coded levels for individual risk contour plots to enhance clarity: the 3×10^{-5} contour is marked in red, indicating a higher risk zone; the 1×10^{-6} contour appears in orange for an intermediate risk level; and the 3×10^{-7} contour is displayed in yellow, indicating a lower risk zone. Areas with acceptable risks of below 3×10^{-7} are represented in green, providing a clear visual distinction between varying levels of risk.

Table 2. Standards for Acceptable Individual Risk in China [27].

Protective Target	Individual Risk Benchmark (Times/Year)	
	New Facilities	Using Facilities
General protective targets of Category III (population < 30)	1×10^{-5}	3×10^{-5}
General protective targets of Category II ($30 \leq$ population < 100)	3×10^{-6}	1×10^{-5}
High sensitivity protective targets; Important protective targets; General protective targets of Category I (population \geq 100)	3×10^{-7}	3×10^{-6}

4. Case Study

The example is based on real data from a specific region in China. The case involves a crude oil storage depot with a total capacity of 6 million m^3 . The tank group consists of six tanks, labeled T1, T2, T3, T4, T5, and T6, each with a capacity of 1 million m^3 . The target tanks for the accident consequence calculations are T1, T2, and T3, within a fire embankment measuring 108 m by 108 m. Environmental conditions include an average annual temperature of 23.3 °C, 80% air humidity, 1.16 kg/m^3 air density, and 101,325 Pa atmospheric pressure. Weather and wind parameters for this area are listed in Table 3 and the specific parameters for the storage tanks are provided in Table 4.

Table 3. Annual average wind frequency.

Time Period	Weather Type	Wind Direction															
		N	NNE	NE	ENE	E	ESE	SE	SSE	S	SSW	SW	WSW	W	WNW	NW	NNW
Daytime	0.1/F	1.2	0.8	1.24	1.63	2.77	2.8	2.1	1.2	1.7	3.3	3.3	2.03	1.6	1.93	2.63	1.64
	1.5/D	1.2	0.8	1.24	1.63	2.77	2.8	2.1	1.2	1.7	3.3	3.3	2.03	1.6	1.93	2.63	1.64
	5/D	1.2	0.8	1.24	1.63	2.77	2.8	2.1	1.2	1.7	3.3	3.3	2.03	1.6	1.93	2.63	1.64
Nighttime	0.1/F	1.2	0.8	1.24	1.63	2.77	2.8	2.1	1.2	1.7	3.3	3.3	2.03	1.6	1.93	2.63	1.64
	1.5/D	1.2	0.8	1.24	1.63	2.77	2.8	2.1	1.2	1.7	3.3	3.3	2.03	1.6	1.93	2.63	1.64
	5/D	1.2	0.8	1.24	1.63	2.77	2.8	2.1	1.2	1.7	3.3	3.3	2.03	1.6	1.93	2.63	1.64

Table 4. Tank and failure parameters.

Tank Parameters		Failure Parameters	
Height (m)	21.8	Leak height (m)	10
Radius (m)	40	Leakage hole diameter (m)	0.025
Material type	Crude oil (dodecane, N-HEXANE)	Failure probability	0.0001
Material quality (kg)	8.65×10^7	Immediate ignition probability	0.065
Number of failed tanks	3	Consequence data (early pool fire, late pool fire, blast overpressure, BLEVE)	Calculated from Algorithm

Currently, countries such as the United Kingdom, the United States, the Netherlands, Norway, Australia, Hong Kong, Singapore, and Malaysia have established individual risk tolerance standards. According to the British Health and Safety Commission and the British Chemical Industry Association, an individual risk exceeding 1.0×10^{-3} per year is deemed unacceptable while an individual risk below 1.0×10^{-5} per year is considered acceptable. In China, individual risk tolerance standards have been formulated according to GB 36894-2018

(Risk criteria for hazardous chemicals production unit and storage installations) [27], which stipulate that individual risk in chemical areas must fall outside the 1.0×10^{-5} contour range (represented by the orange line). In the case of this oil tank area, the maximum individual risk is calculated to be 1.52108×10^{-5} . Using the same parameters, verification analysis was conducted with DNV SAFETI software, resulting in a maximum individual risk value of 1.46583×10^{-5} for the area. The relative error compared to the calculated value is 3.769%. Figure 6, as compared with Table 2, shows that apart from the storage tank area, all other locations remain within the lower risk contour of 3×10^{-6} for individual risk. This indicates that the individual risk to surrounding sensitive targets remains within an acceptable range. Assuming that the failure frequency and ignition probability follow normal distributions with means of 0.0001 and 0.065 and standard deviations of 0.00002 and 0.013, respectively, Monte Carlo simulations were performed to generate 1000 sets of input samples and the corresponding outputs (individual risk maxima). The Cumulative Distribution Function (CDF) is obtained as shown in Figure 8, the red and blue shaded areas represent the 95% confidence intervals. This proves the quality of the data and the reliability of the model output.

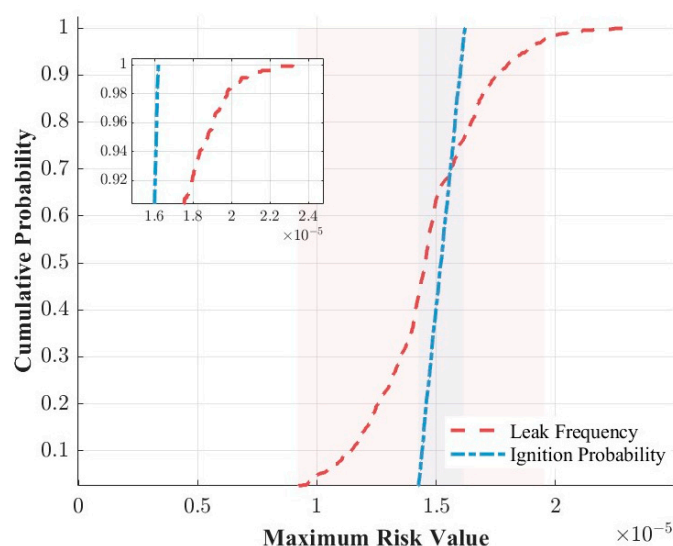


Figure 8. CDF of maximum individual values (1000 samples).

For societal risk, IEC 31010 specifies that the $F-N$ curve should follow the As Low As Reasonably Practicable (ALARP) principle, which divides societal risk into intolerable, ALARP, and broadly acceptable regions using two baseline lines [28]. The baseline selection depends on the risk area, and GB 36894-2018 named benchmarks as “negligible line” and “intolerable line”, and provides acceptable risk criteria for chemical areas [27].

In order to investigate the effects of different input parameters on the model output, three leakage hole diameters (25 mm, 75 mm, and 100 mm) were selected as leakage scenarios for case studies. As shown in Table 5, GB/T37243-2019 provides suggested values for the frequency of small, medium, and large leaks in atmospheric tanks per year. Meanwhile, the accident consequences under these leak scenarios were simulated and substituted into the constructed model to analyze the influence of different input parameters on the results of regional risk calculations.

Table 5. Frequency of leaks from atmospheric storage tanks [17].

	Hole Leakage (0~5 mm)	Medium-Sized Hole Leakage (5~50 mm)	Nozzle Leakage (50~100 mm)
atmospheric storage tank	4×10^{-5}	1×10^{-4}	1×10^{-5}

Figure 9 presents individual risk modeling results for two spill scenarios (corresponding to the first case in Figure 6). The 25 mm aperture scenario shows more frequent spills and higher individual risk peaks, though with a relatively limited range of spill consequences. Conversely, the 75 mm and 100 mm aperture leaks, with identical spill frequencies, exhibit a broader range of spill consequences but lower individual risk peaks, staying below the 1.0×10^{-5} contour level. Figure 10 shows the societal risk modeling outputs for the three spill scenarios, where despite the more frequent 25 mm hole diameters leaks, the overall social risk is smaller and in the ALARP zone due to the relatively smaller impacts of the spill consequences. In contrast, the 75 mm and 100 mm hole diameters leak scenarios have the same frequency of leaks and the societal risk is mostly in the ALARP zone with more similar risk results. However, larger leak apertures imply more severe consequences of the leaks, so that the maximum number of deaths for the 100 mm leak scenario reaches 120, which is more than double that for the 75 mm leak scenario, and the risk is also slightly higher overall.

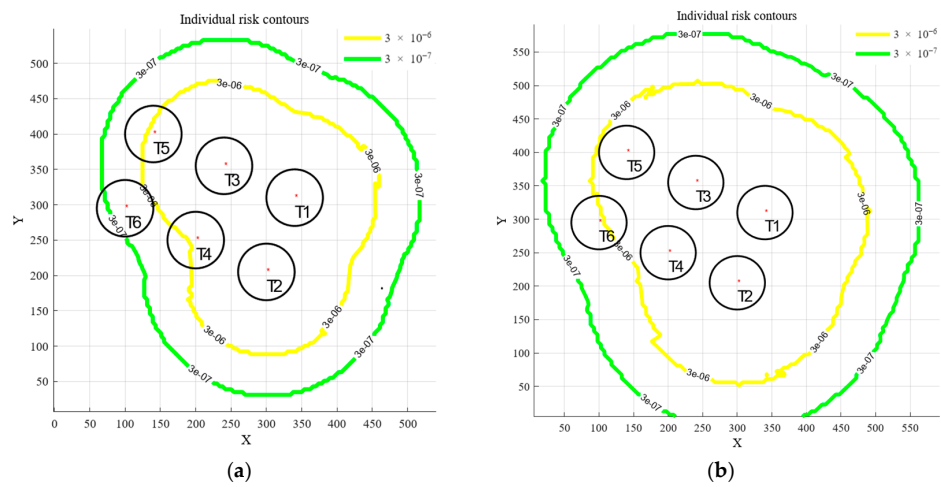


Figure 9. Individual risk outcomes in different spill scenarios. (a) 75 mm hole diameter leak scenarios; (b) 100 mm hole diameter leak scenarios.

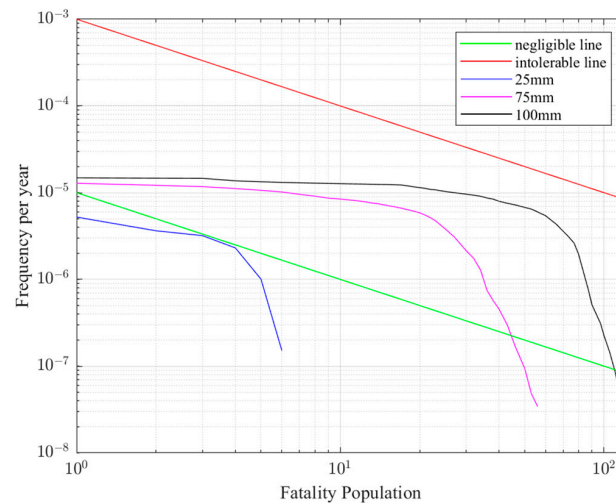


Figure 10. Social risk outcomes in different spill scenarios.

5. Conclusions

In this paper, individual and societal risk models were developed and integrated with weather conditions, grid division methods, and multiple risk superposition calculations to assess complex oil tank leakage scenarios. The key conclusions are as follows:

- (1) The proposed methodology effectively incorporates diurnal variations and weather factors into the risk assessment framework, offering a more nuanced and reliable evaluation of both individual and societal risks. This approach provides a practical tool for engineering applications, particularly in environments like oil tank farms, where maintaining energy security is of paramount importance.
- (2) The model simplifies traditionally complex risk assessment processes, offering a user-friendly and efficient platform for risk analysis. By visually mapping risks and integrating multiple risk factors, it enhances both the accuracy and clarity of assessments, thus contributing to the safer operation of oil tank farms and supporting broader energy supply security.
- (3) While the application of the model to case studies has demonstrated its capability to visually display key quantitative indicators such as individual and societal risk, the accuracy of the results is dependent upon the quality and completeness of the input data. Future research should prioritize improving data acquisition and processing methods to enhance data quality and effectively manage uncertainties. Additionally, expanding the model's application to a wider range of industrial settings will further strengthen its role in safeguarding energy infrastructure. Integrating advanced modeling techniques, such as machine learning algorithms, could also significantly improve the predictive capabilities of risk assessments.

Author Contributions: Conceptualization, Y.Y. and X.Z.; Methodology, S.X., Q.X. and G.C.; Writing—original draft, S.Q. and H.C. All authors have read and agreed to the published version of the manuscript.

Funding: This research was supported by Research on Deepening the Application of Integrity Management for Large Storage Tanks (No. AQWH202208). This research was supported by Deepening research on pipeline risk assessment based on multi-source data (No. AQWH202302), This research was supported by Guangdong Basic and Applied Basic Research Foundation (No. 2024A1515011123).

Data Availability Statement: The original contributions presented in the study are included in the article, further inquiries can be directed to the corresponding author.

Conflicts of Interest: Authors Yufeng Yang and Xixiang Zhang were employed by China Oil & Gas Pipeline Network Corporation. The remaining authors declare that the research was conducted in the absence of any commercial or financial relationships that could be construed as a potential conflict of interest.

Appendix A

Table A1. Parameters used in the calculation procedure.

Name	Units	Description
n	-	Number of tanks that failed
f_s	-	Failure frequency
P_i	-	Ignition probability
E, L	kW/m^2	Thermal radiation matrix for early pool fire and late pool fire, which can be obtained from the pool fire solid flame calculation model
O	bar	The shock wave overpressure matrix, which can be obtained from the vapor cloud explosion (VCE) TNO calculation model
B	kW/m^2	BLEVE thermal radiation matrix
P_{day}	-	Percentage of daytime
P_{night}	-	Percentage of nighttime
P_M	-	Select a weather class, with wind frequency matrix for 16 sectors
G_s	-	Grid size. Enter 100 to generate a grid space of 100×100 units
$step$	m	Grid step, unit length of the grid
$population$	-	Population matrix
P_d	-	The probability of death at the grid point

References

1. CTS News. At Least 17 Dead, 50 Injured in Oil Depot Explosion at Indonesia's State-1un Oil Company. Available online: <https://www.chinatimes.com/realtimenews/20230304001159-260408?chdtv> (accessed on 27 August 2024).

2. Investigation Report on the “5·1” Major Explosion and Fire Accident in Sinochem Liaochem Luxi Hydrogen Peroxide New Material Technology, Co. Available online: http://yj.t.shandong.gov.cn/zw/gk/zdly/aqsc/sgxx/202404/t20240419_4720072.html (accessed on 27 August 2024).
3. Swuste, P.; van Nunen, K.; Reniers, G.; Khakzad, N. Domino Effects in Chemical Factories and Clusters: An Historical Perspective and Discussion. *Process. Saf. Environ. Prot.* **2019**, *124*, 18–30. [[CrossRef](#)]
4. Meng, G.; Hu, H. Research on Multi-Point Monitoring Data Grid Model and Inversion Positioning Method for Gas Leakage in Oil and Gas Stations. *Sustainability* **2024**, *16*, 1638. [[CrossRef](#)]
5. Bartolozzi, V.; Bajardi, S.; Vasile, F.; Marino, S. Safety Integrated Area Analysis: A Recent Case Study. In Proceedings of the Cisap4: 4th International Conference on Safety & Environment in Process Industry, Florence, Italy, 7–10 March 2010; Buratti, S.S., Ed.; Aidic Servizi Srl: Milan, Italy; Volume 19, pp. 457–462.
6. Zhang, H.; Cao, X.; Yuan, X.; Wu, F.; Wang, J.; Zhang, Y.; Li, Q.; Liu, H.; Huang, Z. Study on Thermal Radiation Characteristics and the Multi-Point Source Model of Hydrogen Jet Fire. *Appl. Sci.* **2024**, *14*, 7098. [[CrossRef](#)]
7. Su, J.; Zhang, X.; Zhou, L.; Yin, Y. A Quantitative Analysis Pattern for Regional Risk Conduction. *J. Phys. Conf. Ser.* **2019**, *1419*, 012032. [[CrossRef](#)]
8. Lee, K.; Kang, C. Expansion of Next-Generation Sustainable Clean Hydrogen Energy in South Korea: Domino Explosion Risk Analysis and Preventive Measures Due to Hydrogen Leakage from Hydrogen Re-Fueling Stations Using Monte Carlo Simulation. *Sustainability* **2024**, *16*, 3583. [[CrossRef](#)]
9. Jonkman, S.N.; Jongejan, R.; Maaskant, B. The Use of Individual and Societal Risk Criteria Within the Dutch Flood Safety Policy—Nationwide Estimates of Societal Risk and Policy Applications. *Risk Anal. Int. J.* **2011**, *31*, 282–300. [[CrossRef](#)] [[PubMed](#)]
10. Park, B.; Kim, Y.; Lee, K.; Paik, S.; Kang, C. Risk Assessment Method Combining Independent Protection Layers (IPL) of Layer of Protection Analysis (LOPA) and RISKCURVES Software: Case Study of Hydrogen Refueling Stations in Urban Areas. *Energies* **2021**, *14*, 4043. [[CrossRef](#)]
11. Kwak, H.; Kim, M.; Min, M.; Park, B.; Jung, S. Assessing the Quantitative Risk of Urban Hydrogen Refueling Station in Seoul, South Korea, Using SAFETI Model. *Energies* **2024**, *17*, 867. [[CrossRef](#)]
12. Abdolhamidzadeh, B.; Abbasi, T.; Rashtchian, D.; Abbasi, S.A. Corrigendum to “A New Method for Assessing Domino Effect in Chemical Process Industry” [*J. Hazard. Mater.* **2010**, *182*, 416–426]. *J. Hazard. Mater.* **2010**, *184*, 877. [[CrossRef](#)] [[PubMed](#)]
13. Zhao, M.; Liu, X. Reprint of: Regional Risk Assessment for Urban Major Hazards Based on GIS Geoprocessing to Improve Public Safety. *Saf. Sci.* **2017**, *97*, 112–119. [[CrossRef](#)]
14. Rajeev, K.; Soman, S.; Renjith, V.; George, P. Human Vulnerability Mapping of Chemical Accidents in Major Industrial Units in Kerala, India for Better Disaster Mitigation. *Int. J. Disaster Risk Reduct.* **2019**, *39*, 101247. [[CrossRef](#)]
15. Tahmid, M.; Dey, S.; Syeda, S.R. Mapping Human Vulnerability and Risk Due to Chemical Accidents. *J. Loss Prev. Process Ind.* **2020**, *68*, 104289. [[CrossRef](#)]
16. Dormohammadi, A.; Zarei, E.; Delkhosh, M.B.; Gholami, A. Risk Analysis by Means of a QRA Approach on a LPG Cylinder Filling Installation. *Process Saf. Prog.* **2014**, *33*, 77–84. [[CrossRef](#)]
17. GB/T 37243-2019; Determination Method of External Safety Distance for Hazardous Chemicals Production Units and Storage Installations. National Standards of People’s Republic of China: Beijing, China, 2019. Available online: <https://www.chinesestandard.net/Related.aspx/GBT37243-2019> (accessed on 20 September 2024).
18. SH/T 3226-2024; Standards for Quantitative Analysis of Petrochemical Processes Risks. Ministry of Industry and Information Technology: Beijing, China, 2024. Available online: http://www.standardcn.com/standard_bp/BPG_ReadFile.asp?FID=20861 (accessed on 20 September 2024).
19. AQ/T 3046-2013; Guidelines for Quantitative Risk Assessment of Chemical Enterprises. National Standardization Technical Committee of Safety Production Technical Committee on Chemical Safety: Beijing, China, 2013. Available online: <https://www.chinesestandard.net/Related.aspx/AQT3046-2013> (accessed on 20 September 2024).
20. DNV. The MPACT Risk Model Theory. Available online: https://myworkspace.dnv.com/download/public/phast/technical_documentation/09_risk/MPACT%20Risk%20Model%20Theory.pdf (accessed on 20 September 2024).
21. ISO 31000:2018; Risk Management—Guidelines. ISO: Geneva, Switzerland, 2018. Available online: <https://www.iso.org/standard/65694.html> (accessed on 20 September 2024).
22. Guelzim, A.; Chakir, B.A.; Ettahir, A.; Mbarki, A. Use of Statistical Tools for Comparison between Different Analytical and Semi-Empirical Models of the Bleve Fireball. *Front. Heat Mass Transf.* **2023**, *21*, 125–140. [[CrossRef](#)]
23. Zhao, J.; Wu, M.; Lu, H.; Li, G.; Xu, Y.; Tian, M. Quantitative Risk Assessment of an Oil-Gas-Hydrogen-Electricity Integrated Energy Station in China. *ACS Omega* **2024**, *9*, 38887–38896. [[CrossRef](#)] [[PubMed](#)]
24. Carboni, M.; Pio, G.; Mocellin, P.; Vianello, C.; Maschio, G.; Salzano, E. On the Flash Fire of Stratified Cloud of Liquefied Natural Gas. *J. Loss Prev. Process Ind.* **2022**, *75*, 104680. [[CrossRef](#)]
25. Tsukada, R.I.; Shiguemoto, D.A.; Vianna, S.S. The TNO Multi-Energy Method Combined to Mathematical Programming and Computational Fluid Dynamics for Optimisation of Gas Detectors. *J. Loss Prev. Process Ind.* **2023**, *83*, 105035. [[CrossRef](#)]
26. Shen, G.; Zhou, K.; Wu, F.; Jiang, J.; Dou, Z. A Model Considering the Flame Volume for Prediction of Thermal Radiation from Pool Fire. *Fire Technol.* **2019**, *55*, 129–148. [[CrossRef](#)]

27. *GB 36894-2018*; Risk Criteria for Hazardous Chemicals Production Unit and Storage Installations. National Standards of People's Republic of China: Beijing, China. Available online: <https://www.chinesestandard.net/Related.aspx/GB36894-2018> (accessed on 20 September 2024).
28. *IEC 31010:2019*; Risk Management—Risk Assessment Techniques. ISO: Geneva, Switzerland, 2019. Available online: <https://www.iso.org/standard/72140.html> (accessed on 30 June 2019).

Disclaimer/Publisher's Note: The statements, opinions and data contained in all publications are solely those of the individual author(s) and contributor(s) and not of MDPI and/or the editor(s). MDPI and/or the editor(s) disclaim responsibility for any injury to people or property resulting from any ideas, methods, instructions or products referred to in the content.